

BT-3551

Research and Development of Rigid, Rising, Radar Reflective Balloons:
Vol. I The Wind Response Error of an Ascending Balloon
Under Consideration of Apparent Mass

G.T. Schjeldahl Co.

H.G. Heinrich, et al

24 Jul 1963

G. T. SCHJELDAHL COMPANY
NORTHFIELD, MINNESOTA

July 24, 1953

RESEARCH AND DEVELOPMENT OF
RIGID, RISING, RADAR REFLECTIVE BALLOONS

Vol 1

VOLUME I

THE WIND RESPONSE ERROR OF AN ASCENDING BALLOON
UNDER CONSIDERATION OF APPARENT MASS

G. T. SCHJELDAHL COMPANY
Northfield, Minnesota

Final Report on
CONTRACT AF 19(628)-2393

PREPARED FOR

AIR FORCE CAMBRIDGE RESEARCH LABORATORIES
OFFICE OF AEROSPACE RESEARCH
LAURENCE G. HANSCOM FIELD
BEDFORD, MASSACHUSETTS

THE WIND RESPONSE ERROR
OF AN ASCENDING BALLOON UNDER
CONSIDERATION OF THE APPARENT MASS

H. G. Heinrich
L. W. Rust
E. L. Haak
R. J. Niccum

University of Minnesota
Minneapolis, Minnesota

The
Project was Sponsored by
G. T. Schjeldahl Company, Northfield, Minnesota

ABSTRACT

An attempt has been made to analyze several factors which contribute to the difference of motion between an ascending balloon and actual wind profiles. Two analytical solutions are presented which give the wind response error of the balloon as a function of the altitude, the wind profile, and the location of the balloon within the wind shear layer. These solutions, both including and neglecting the apparent mass, agree well with computer solutions. The apparent mass of actual balloons has been measured.

LIST OF TABLES

<u>Table No</u>		<u>Page</u>
I.	Experimental Results for a Freely Descending Sphere at Four Reynolds Numbers	39

LIST OF FIGURES

<u>Figure No</u>		<u>Page</u>
1.	Wind Shear and Balloon Velocity (With Apparent Mass Factor of 0 and 0.5) As a Function of Altitude ($h_0=15,000$ ft, $\alpha=0.14$) . .	22
2.	Wind Shear and Balloon Velocity (With Apparent Mass Factor of 0 and 0.5) As a Function of Altitude ($h_0=15,000$ ft, $\alpha=0.28$) . .	23
3.	Wind Shear and Balloon Velocity (With Apparent Mass Factor of 0 and 0.5) As a Function of Altitude ($h_0=55,000$ ft, $\alpha=0.28$) . .	24
4.	Forces Acting on the Experimental System During Descent	27
5.	Schematic Diagram of Test Apparatus and Arrangement	31
6.	Photograph of Inflated 2.44 Meter Balloon (24)Gores)	32
7.	Photograph of Inflated 2 Meter Balloon (12 Gores)	33
8.	Inflated 12 Gore Balloon Showing Non-sphericity of Cross Section	34
9.	Sample Oscillograph Trace	38
10.	Reynolds Number Vs Apparent Mass Factor for Super-Pressured Mylar Balloons	43

LIST OF SYMBOLS

ρ	- local air density
ρ_G	- density of enclosed gas
α	- wind gradient = $\delta V_{\infty}/h$
a_0	- acceleration of balloon during its fall
B	- buoyancy of balloon = $\rho \cdot \text{Vol} \cdot g$
C_D	- drag coefficient
D	- aerodynamic drag
F	- net downward force of balloon system
g	- acceleration of gravity = 32.2 ft/sec ²
n	- ratio $\frac{dV}{dV/g}$; exponent
h	- altitude
K	- apparent mass factor = $\frac{\text{apparent mass}}{\text{mass of air displaced}}$
m_G	- mass of enclosed gas
m_R	- remaining mass = W_R/g
m_S	- mass of falling balloon structure and fittings
m'	- apparent mass
M'	- apparent weight = $m'g$
P	- atmospheric pressure
P_G	- pressure of enclosed gas
R	- gas constant of air
R_G	- gas constant of enclosed gas
S	- projected area
t	- time

I. INTRODUCTION

The satisfactory recording of magnitude and direction of wind at various altitudes by means of an ascending balloon depends among other things upon the capability of the balloon to assume the velocity of the surrounding air in the shortest possible time. The difference between the actual air movement and the respective motion of the ascending balloon is called "response error" (Ref 1), and a balloon which would assume instantaneously the actual air velocity, would have a "zero response error."

Physically the phenomenon of response error can be described as follows. When the ascending balloon enters into a layer of horizontal wind which has a nearly constant velocity versus altitude, the balloon has to be accelerated until the relative velocity between balloon and surrounding air becomes insignificant. During the period of acceleration, we will have a decreasing response error which approaches zero when the balloon velocity is practically equal to the wind velocity.

If an ascending balloon enters into horizontal wind which increases in magnitude with altitude, the balloon has to be steadily accelerated while it passes through the wind layer. This results in a response error depending on the variation of the wind with altitude.

These simple considerations indicate that a balloon

with a high response error may lead to faulty information about the wind pattern, and in the following, an attempt will be made to analyze several reasons which contribute to the response error.

The movement of the ascending balloon is governed by the equation of motion which represents essentially Newton's Second law. A closer study of this equation indicates that a balloon will follow the actual air movements rapidly if its speed of ascent is low, its ratio of weight to surface area is small, and if its apparent mass is a minimum.

Because of certain conveniences, spherical balloons are mostly used for this purpose and this selection establishes certain aspects in regard to drag coefficient, Reynolds number effect, and the magnitude of the apparent mass. This, however, does not mean that spherical balloons are really the best objects for this purpose.

The question of how light a balloon per unit of cross section area can be built is a problem of balloon fabrication. The apparent mass of a spherical balloon is proportional to the third power of the radius and since the apparent mass tends to increase the response error, the smallest balloon possible should be used. However, the balloon has to be large enough to climb to the required altitude in the prescribed time and must also be visible on the radar

screen. Therefore, the entire matter of designing the most suitable balloon is an optimization process in which the weight per unit of projected area, the apparent mass, the drag coefficient, and the balloon buoyancy are the principal components.

The pursuit of this total problem exceeds the scope of this study, which shall be limited to an analysis of the trajectory and to a measurement of the apparent mass of actual balloons.

The trajectory analysis shown in Section II is pursued in a closed-form solution and a first approximation both with and without the effect of apparent mass. The results of these efforts are compared with earlier publications (Ref 2). An additional calculation is then performed which includes the term of the apparent mass of a sphere derived from potential flow theory.

In the third section, measurements of the apparent mass of actual balloons are described. The influence of the Reynolds number upon the apparent mass appears to be important since the magnitude of the apparent mass is a function of the flow pattern related to a subcritical or supercritical Reynolds number operation. The importance of this investigation is emphasized through the fact that most ascending spheres used for the detection of wind operate in the supercritical, transitional, and subcritical Reynolds number regions.

II. TRAJECTORY CALCULATION

A. Development of the Equations of Motion

The manner in which an ascending balloon follows the actual horizontal movement of air, and wind follows from the equation of motion of the balloon. Newton's second law may be written symbolically as:

$$\Sigma \vec{F} = m_{\text{tot}} \frac{d\vec{V}}{dt}, \quad (1)$$

where

- m_{tot} = total mass of the balloon
- \vec{V} = absolute velocity of the balloon
- $\Sigma \vec{F}$ = sum of all external forces acting on the balloon.

We choose Z as the vertical and X as the horizontal direction. The motion of the balloon is assumed to be restricted to the X-Z plane.

The total mass (m_{tot}) of Eqn 1 consists of:

- 1) m_S = mass of the balloon material, including valves, hardware, etc.
- 2) m_G = mass of the gas within the balloon
- 3) m' = apparent mass.

The apparent mass arises from the transfer of kinetic energy from the sphere to the surrounding air and for ideal fluid has been found to be equal to half the mass of air

displaced by the balloon (Ref 3).

The external forces acting on the balloon are aerodynamic drag, gravity, and buoyancy forces. Mathematically, this may be expressed as:

$$\Sigma \vec{F} = \vec{D} + \vec{W} + \vec{B} \quad , \quad (2)$$

where

\vec{D} = aerodynamic drag

\vec{W} = weight of balloon material plus included gas

\vec{B} = buoyancy.

We must here differentiate between three different velocities. The absolute velocity of air is denoted by \vec{V}_w , that of the balloon by \vec{V} , and the relative velocity of the balloon with respect to the air by \vec{V}_r . By this definition of \vec{V}_r we have:

$$\vec{V}_r = \vec{V} - \vec{V}_w \quad . \quad (3)$$

Writing the velocities in terms of components, we have

$$\begin{aligned} \vec{V} &= V_x \hat{i} + V_z \hat{k} \\ \vec{V}_w &= V_{xw} \hat{i} \end{aligned} \quad (4)$$

We have here assumed that the wind has no vertical component.

Thus, we find from Eqns 3 and 4 that:

$$\vec{V}_r = (V_x - V_{xw}) \hat{i} + V_z \hat{k} \quad . \quad (5)$$

We are now in a position to write expressions for the external forces acting on the balloon. The drag force

is conventionally expressed as:

$$\vec{D} = -C_{D2} \frac{1}{2} \rho V_r^2 S \hat{\tau} \quad (6)$$

where

C_D = coefficient of drag

ρ = air density

S = cross sectional area of balloon (also the projected area)

$\hat{\tau}$ = unit vector in the direction of the relative velocity (V_R),

and $\hat{\tau}$ may thus be expressed as:

$$\hat{\tau} = \frac{\vec{V}_r}{|\vec{V}_r|} ; \quad (7)$$

consequently we find:

$$\vec{D} = -C_{D2} \frac{1}{2} \rho V_r S \vec{V}_r . \quad (8)$$

The gravity force is given by:

$$\vec{W} = -(m_s + m_o) g \hat{k} . \quad (9)$$

Finally, the buoyant force is given by the weight of air displaced by the balloon. Thus:

$$\vec{B} = \rho \text{Vol} \hat{k} g , \quad (10)$$

where

Vol = volume of balloon

g = acceleration of gravity = 32.2 ft/sec²

\hat{k} = unit vector in the Z direction.

We therefore obtain the resultant of the forces:

$$\Sigma \vec{F} = -C_D \frac{1}{2} \rho S V_r \vec{V}_r - (m_s + m_g) g \hat{k} + \rho g \text{Vol} \hat{k} . \quad (11)$$

Using relation (5) in (11) we find:

$$\vec{F} = C_D \frac{1}{2} \rho S V_r [(V_x - V_{xw}) \hat{i} + V_z \hat{k}] - (m_s + m_g) g \hat{k} + \rho g \text{Vol} \hat{k} . \quad (12)$$

Substituting this relation, along with Eqn 4, into Eqn 1 yields:

$$(m_s + m_g + m')(\dot{V}_x \hat{i} + \dot{V}_z \hat{k}) = -C_D \frac{1}{2} \rho S V_r [(V_x - V_{xw}) \hat{i} + V_z \hat{k}] - (m_s + m_g) g \hat{k} + \rho \text{Vol} g \hat{k} . \quad (13)$$

Or, in terms of the component directions:

$$(m_s + m_g + m') \dot{V}_x = -C_D \frac{1}{2} \rho S V_r (V_x - V_{xw}) \quad (14)$$

$$(m_s + m_g + m') \dot{V}_z = -C_D \frac{1}{2} \rho S V_r V_z - (m_s + m_g) g + \rho g \text{Vol} , \quad (15)$$

where the magnitude of V_R is given by:

$$V_r = \sqrt{(V_x - V_{xw})^2 + V_z^2} . \quad (16)$$

These equations correspond to Eqns 9a and 9b of Ref 2, the only difference being that Ref 2 did not consider the effects of apparent mass. Since the apparent mass constitutes a fairly large percentage of the physical mass, it is necessary that this be taken into account for accurate results. A comparison of the solution which includes apparent mass with one where it is neglected is presented in Section C.

The mass of gas within the balloon can be expressed as:

$$m_G = \rho_G \text{Vol} , \quad (17)$$

where ρ_G = density of the gas within the balloon.

We now will proceed to represent the internal gas density (ρ_G) in terms of the external air density. The internal gas density is given by the perfect gas law as:

$$\rho_G = \frac{P_G}{R_G T_G} . \quad (18)$$

We assume that a pressure sensing valve is used such that the difference between the internal and external pressures is kept constant, or:

$$P_G - P = \Delta P = \text{constant}$$

or

$$P_G = P + \Delta P . \quad (19)$$

Substituting Eqn 19 into Eqn 18 yields:

$$\rho_G = \frac{P}{R_G T_G} + \frac{\Delta P}{R_G T_G} . \quad (20)$$

Assuming that the balloon is in thermal equilibrium with the surrounding air, we may assume that $T_G = T_{\text{air}} = T$ and write:

$$\rho_G = \frac{P}{R_G T} + \frac{\Delta P}{R_G T} . \quad (21)$$

Since we may write (for the ambient air):

$$P = \rho R T \quad , \quad (22)$$

we obtain:

$$\rho_G = \left(\frac{R}{R_G} \right) \rho + \left(\frac{\Delta P}{T R_G} \right) \quad . \quad (23)$$

Substituting Eqn 23 into Eqn 17 gives:

$$m_G = \left(\frac{R}{R_G} \right) \rho \text{Vol.} + \left(\frac{\Delta P}{T R_G} \right) \text{Vol.} \quad (24)$$

The apparent mass is conventionally represented as:

$$m^i = K \rho \text{Vol} \quad (25)$$

(Note: for potential flow, we have $K = \frac{1}{2}$.)

Utilizing relations (24) and (25) in (14) and (15) yields:

$$(m_s + \frac{R}{R_G} \rho \text{Vol} + \frac{\Delta P}{T R_G} \text{Vol} + K \rho \text{Vol}) \dot{V}_x = \frac{C_D \rho S V_r}{2} (V_{xw} - V_x) \quad (14a)$$

$$\begin{aligned} (m_s + \frac{R}{R_G} \rho \text{Vol} + \frac{\Delta P}{T R_G} \text{Vol} + K \rho \text{Vol}) \dot{V}_z = & - \frac{C_D \rho S V_r}{2} V_z - \\ & - (m_s + \frac{R}{R_G} \rho \text{Vol} + \frac{\Delta P}{T R_G} \text{Vol}) g + \rho g \text{Vol} . \end{aligned} \quad (15a)$$

These may be rewritten in terms of design parameters as:

$$(C_1 + C_2 \rho) \dot{V}_x = \frac{C_D S \rho V_r}{2} (V_{xw} - V_x) \quad (26)$$

$$(C_1 + C_2 \rho) \dot{V}_z = - \frac{C_D S \rho V_r V_z}{2} - (C_1 + \frac{R}{R_G} \text{Vol} \rho) g + \rho g \text{Vol} , \quad (27)$$

where:

$$C_1 = m_s + \frac{\Delta P}{T R_G} \text{ Vol}$$

$$C_2 = \left(\frac{R}{R_G} + K \right) \text{ Vol} .$$

We shall attempt to obtain a closed-form solution for these equations in the following section.

B. Solutions of the Governing Equations

We shall examine two solutions in this section. The first shall be a more or less "exact" solution which accounts for the variation in air density over the altitude interval under consideration. The second will assume a constant air density over this interval and proves to be more easily evaluated. Finally, the two solutions will be compared and some general results shown.

We will here concern ourselves with shear layers which are not extremely thick, e.g., altitude intervals less than 500 ft. For this size of interval, we may safely assume that the vertical velocity remains constant. Thus, $\dot{V}_z \cong 0$ and we may solve Eqn 27 for V_R and obtain:

$$V_r = \frac{\left[\rho \left(1 - \frac{R}{R_G} \right) - \frac{\Delta P}{T R_G} \right] \text{Vol } g - m_s g}{\frac{C_D S}{2} \rho V_z} . \quad (29)$$

Substituting this relation into Eqn 26 yields:

$$(C_1 + C_2 \rho) \dot{V}_x = \frac{(V_{xw} - V_x)}{V_z} (C_3 \rho - C_1) g, \quad (30)$$

where:

$$C_3 = (1 - \frac{R}{R_G}) \text{ Vol}. \quad (31)$$

We may expand \dot{V}_x as:

$$\dot{V}_x = \frac{dV_x}{dt} = \frac{dV_x}{d\rho} \frac{d\rho}{dt} = \frac{dV_x}{d\rho} \frac{d\rho}{dh} \frac{dh}{dt}. \quad (32)$$

One recognizes that $\frac{dh}{dt} = V_z$. Thus, we have:

$$\dot{V}_x = V_z \frac{d\rho}{dh} \frac{dV_x}{d\rho}. \quad (33)$$

In order to evaluate $\frac{d\rho}{dh}$, we make use of the exponential density law given by:

$$\frac{\rho}{\rho_0} = e^{-\beta(h-h_0)}, \quad (34)$$

where:

ρ = air density at altitude h

ρ_0 = air density at altitude h_0 (h_0 is the altitude of beginning of shear layer)

β = logarithmic density slope.

Differentiating, we obtain:

$$\frac{d\rho}{dh} = -\rho_0 \beta e^{-\beta(h-h_0)} = -\beta \rho. \quad (35)$$

Substituting this relation in Eqn 33 we find:

$$\dot{V}_x = -\beta \rho V_z \frac{dV_x}{d\rho}. \quad (36)$$

Utilizing this equation, relation (30) becomes, after rearranging:

$$\frac{dV_x}{d\rho} = \frac{(V_{xw} - V_x)}{\beta \rho V_z^2} \left[\frac{C_1 - C_3 \rho}{C_1 + C_2 \rho} \right] g \quad . \quad (37)$$

In view of the objective to find the difference between the wind and balloon velocity (wind response error), it is convenient to introduce $\frac{dV_{xw}}{d\rho}$ at this time. Subtracting this quantity from both sides of Eqn 37 yields:

$$\frac{d(V_x - V_{xw})}{d\rho} = \frac{(V_{xw} - V_x)}{\beta \rho V_z^2} \left[\frac{C_1 - C_3 \rho}{C_1 + C_2 \rho} \right] g - \frac{dV_{xw}}{d\rho} \quad ,$$

or, rearranging:

$$\frac{d(V_{xw} - V_x)}{d\rho} + \frac{g}{\beta \rho V_z^2} \left[\frac{C_1 - C_3 \rho}{C_1 + C_2 \rho} \right] (V_{xw} - V_x) = \frac{dV_{xw}}{d\rho} \quad . \quad (38)$$

This equation has the form:

$$\frac{dy}{dx} + f(x)y = g(x) \quad . \quad (39)$$

The integrating factor for the left side of this equation is given by:

$$e^{\int f(x) dx} \quad . \quad (40)$$

Multiplying both sides of Eqn 39 by Eqn 40 gives:

$$e^{\int f(x) dx} \frac{dy}{dx} + e^{\int f(x) dx} f(x)y = g(x) e^{\int f(x) dx} \quad . \quad (41)$$

One recognizes that:

$$\frac{d}{dx} \left[e^{\int f(x) dx} y \right] = e^{\int f(x) dx} \frac{dy}{dx} + f(x) e^{\int f(x) dx} y \quad .$$

Thus Eqn 41 becomes.

$$\frac{d}{dx} \left[e^{\int f(x) dx} y \right] = g(x) e^{\int f(x) dx},$$

or

$$e^{\int f(x) dx} y = \int g(x) e^{\int f(x) dx} dx. \quad (42)$$

For our case, the integrating factor is:

$$\begin{aligned} e^{\int \frac{g}{\beta \rho V_z^2} \left[\frac{C_1 + C_2 \rho}{C_1 + C_2 \rho} \right] d\rho} &= e^{\ln \left[\frac{(C_1 + C_2 \rho)^{\frac{C_3 + 1}{C_2}}}{\rho} \right]^{-\frac{g}{\beta V_z^2}}} \\ &= \left[\frac{(C_1 + C_2 \rho)^{\frac{C_3 + 1}{C_2}}}{\rho} \right]^{-\frac{g}{\beta V_z^2}}. \end{aligned}$$

We therefore obtain:

$$\left[\frac{(C_1 + C_2 \rho)^{\frac{C_3 + 1}{C_2}}}{\rho} \right]^{-\frac{g}{\beta V_z^2}} (V_{xw} - V_x) \bigg|_{\rho_0}^{\rho} = \int_{\rho_0}^{\rho} \left[\frac{(C_1 + C_2 \rho')^{\frac{C_3 + 1}{C_2}}}{\rho'} \right]^{-\frac{g}{\beta V_z^2}} \left(\frac{dV_{xw}}{d\rho'} \right) d\rho'$$

where

$\rho' =$ a so-called "dummy variable"

$\rho_0 =$ air density at beginning of altitude interval.

We impose the condition that at h_0 (where $\rho = \rho_0$),

$V_{xw} = V_x = 0$. Thus we have:

$$\left[\frac{(C_1 + C_2 \rho)^{\frac{C_3 + 1}{C_2}}}{\rho} \right]^{-\frac{g}{\beta V_z^2}} (V_{xw} - V_x) = \int_{\rho_0}^{\rho} \left[\frac{(C_1 + C_2 \rho')^{\frac{C_3 + 1}{C_2}}}{\rho'} \right]^{-\frac{g}{\beta V_z^2}} \left[\frac{dV_{xw}}{d\rho'} \right] d\rho'. \quad (43)$$

Solving for $(V_{xw} - V_x)$ we find:

$$V_{xw} - V_x = \int_{\rho_0}^{\rho} \left[\frac{C_1 + C_2 \rho'}{C_1 + C_2 \rho} \right]^{-\left(\frac{C_3}{C_2} + 1\right) C_4} \left[\frac{\rho}{\rho'} \right]^{-C_4} \frac{dV_{xw}}{d\rho'} d\rho', \quad (44)$$

where $C_4 = \frac{g}{\beta V_z^2}$.

We now make a change of variables as:

$$\eta = \frac{\rho'}{\rho_0}. \quad (45)$$

The new limits of integration become 1 and $\frac{\rho_0}{\rho}$ and we obtain:

$$V_{xw} - V_x = - \int_1^{\frac{\rho_0}{\rho}} \left[\frac{C_1 + C_2 \rho}{C_1 + C_2 \rho \eta} \right]^{\frac{C_3}{C_2} + 1} \eta^{C_4} \frac{dV_{xw}}{d\eta} d\eta. \quad (46)$$

We will finally be interested in the case where V_{xw} has a linear variation with altitude. For the present, we shall consider the more general case where

$$V_{xw} = \alpha (h - h_0)^n \quad (47)$$

We must express V_{xw} as a function of η for use in Eqn 46. Writing the exponential density law in terms of the dummy variable, ρ' , we obtain:

$$\frac{\rho'}{\rho_0} = e^{-\beta(h' - h_0)}$$

or

$$h' - h_0 = \frac{\ln \rho_0 / \rho'}{\beta}.$$

Thus, we have:

$$V_{xw} = \alpha \left[\frac{\ln \rho_0 / \rho'}{\beta} \right]^n, \quad (48)$$

which may be rewritten (since $\frac{\rho}{\rho} = \eta$) as:

$$V_{xw} = \alpha \left[\frac{\ln \frac{\rho_0/\rho}{\beta/\eta}}{\beta} \right]^n = \alpha \left[\frac{\ln \frac{\rho_0}{\beta/\eta}}{\beta} \right]^n. \quad (48a)$$

Differentiating, we find:

$$\frac{d V_{xw}}{d \eta} = - \frac{\alpha n}{\beta^n \eta} \ln^{n-1} \frac{\rho_0}{\beta/\eta}. \quad (49)$$

Substituting Eqn 49 into Eqn 46, we finally obtain:

$$V_{xw} - V_x = \int_1^{\rho_0/\beta} \left[\left(\frac{C_1 + C_2 \rho}{C_1 + C_2 \rho \eta} \right)^{\frac{C_3}{C_2} + 1} \eta \right]^{C_4} \frac{\alpha n}{\beta^n \eta} \ln^{n-1} \frac{\rho_0}{\beta/\eta} d \eta. \quad (50)$$

This equation gives an integral relation for $V_{xw} - V_x$ for any given shear profile of the form shown in Eqn 47.

We now specialize to a linear profile by letting

$n = 1$ and obtain:

$$V_{xw} - V_x = \frac{\alpha}{\beta} \int_1^{\rho_0/\beta} \left[\left(\frac{C_1 + C_2 \rho}{C_1 + C_2 \rho \eta} \right)^{\frac{C_3}{C_2} + 1} \eta \right]^{C_4} \frac{d \eta}{\eta}, \quad (51)$$

which may be rewritten as:

$$V_{xw} - V_x = \frac{\alpha}{\beta} \int_1^{\rho_0/\beta} \left[\left(\frac{1 + C_5 \rho}{1 + C_5 \rho \eta} \right)^{\frac{C_3}{C_2} + 1} \eta \right]^{C_4} \frac{d \eta}{\eta}, \quad (52)$$

where:

$$\left. \begin{aligned} C_5 &= \frac{C_2}{C_1} = \frac{(K + \frac{R}{R_G}) Vol}{m_s + \frac{\Delta P}{TR_G} Vol} \\ \frac{C_3}{C_2} + 1 &= \frac{1 + K}{R/R_G + K} \\ C_4 &= \frac{g}{\beta V_z^2} \end{aligned} \right\} \quad (53)$$

We must now integrate relation (52). Since we are considering altitude intervals no larger than 500 ft, the upper limit of the integral in relation (52) is quite close to unity. For example, from Ref 4 we have: $\beta = \frac{1}{23,000}$ and therefore $\frac{\rho_o}{\rho} = e^{-\frac{h-h_o}{23,000}} = e^{-\frac{500}{23,000}}$ for $h = h_o = 500$ and thus we have $\frac{\rho_o}{\rho} = 1.022$. Numerical examination of the term within the bracket in Eqn 52 reveals that this quantity is almost a linear function of η in the range $\eta = 1$ to $\eta = 1.022$. Thus, we may approximate this by a Taylor's series about $\eta = 1$ with all but the first two terms neglected. That is, we may express

$$g(\eta) = \left(\frac{1 + C_5 \rho}{1 + C_5 \rho \eta} \right)^{\frac{C_3 + 1}{C_2}} \eta$$

by:

$$g(\eta) = g(\eta=1) + g'(\eta=1)(\eta-1)$$

One easily finds through differentiation that:

$$g'(\eta=1) = 1 - \left(\frac{C_3}{C_2} + 1 \right) \frac{C_5 \rho}{1 + C_5 \rho}$$

and therefore:

$$g(\eta) = 1 + \left[1 - \left(\frac{C_3}{C_2} + 1 \right) \frac{C_5 \rho}{1 + C_5 \rho} \right] (\eta - 1) \quad (54)$$

Substituting this in relation (52) we find:

$$V_{xw} - V_x = \frac{\alpha}{\beta} \int_1^{\eta_p} \left\{ 1 + \left[1 - \left(\frac{C_3}{C_2} + 1 \right) \frac{C_5 \rho}{1 + C_5 \rho} \right] (\eta - 1) \right\}^{C_4} \frac{d\eta}{\eta}$$

Since $\eta \leq 1$ over the range of integration we may replace $\frac{d\eta}{\eta}$ by $d\eta$ and obtain:

$$V_{xw} - V_x = \frac{\alpha}{\beta} \int_1^{R/\rho} \left\{ 1 + \left[1 - \left(\frac{C_3}{C_2} + 1 \right) \frac{C_5 \rho}{1 + C_5 \rho} \right] (\eta - 1) \right\}^{C_4} d\eta. \quad (55)$$

This may be integrated directly to give:

$$V_{xw} - V_x = \frac{\alpha}{\beta (C_4 + 1) \left[1 - \left(\frac{C_3}{C_2} + 1 \right) \frac{C_5 \rho}{1 + C_5 \rho} \right]} \left\{ \left[1 + \left[1 - \left(\frac{C_3}{C_2} + 1 \right) \frac{C_5 \rho}{1 + C_5 \rho} \right] (\eta - 1) \right]^{C_4 + 1} \right\} \bigg|_1^{\frac{\rho_0}{\rho}} \quad (56)$$

or:

$$V_{xw} - V_x = \frac{\alpha}{\beta (C_4 + 1) \left[1 - \left(\frac{C_3}{C_2} + 1 \right) \frac{C_5 \rho}{1 + C_5 \rho} \right]} \left\{ \left[1 + \left[1 - \left(\frac{C_3}{C_2} + 1 \right) \frac{C_5 \rho}{1 + C_5 \rho} \right] \left(\frac{\rho_0}{\rho} - 1 \right) \right]^{C_4 + 1} - 1 \right\}. \quad (57)$$

For the second solution we assume ρ is constant over the altitude interval and write:

$$\dot{V}_x = \frac{dV_x}{dh} \frac{dh}{dt} = V_z \frac{dV_x}{dh}. \quad (58)$$

Substituting this in Eqn 30 and rearranging yields:

$$\frac{dV_x}{dh} = \left[\frac{V_{xw} V_x}{V_z^2} \right] \left[\frac{C_3 \rho_0 - C_1}{C_2 \rho_0 + C_1} \right] g, \quad (59)$$

where ρ_0 = air density at $h = h_0$ (lower edge of shear layer).

Subtracting $\frac{dV_{xw}}{dh}$ from both sides of this equation and rearranging gives:

$$\frac{d(V_{xw} - V_x)}{dh} + \left[\frac{C_3 \rho_0 - C_1}{C_2 \rho_0 + C_1} \right] \frac{g}{V_z^2} (V_{xw} - V_x) = \frac{dV_{xw}}{dh}. \quad (60)$$

Assuming that V_z and ρ are constant, we find the integrating factor to be:

$$e^{\int \frac{C_3 \rho_o - C_1}{C_2 \rho_o + C_1} \frac{g}{V_z^2} dh} = e^{\frac{C_3 \rho_o - C_1}{C_2 \rho_o + C_1} \frac{g}{V_z^2} \int dh} = e^{\frac{C_3 \rho_o - C_1}{C_2 \rho_o + C_1} \frac{gh}{V_z^2}}. \quad (61)$$

Thus Eqn 60 becomes:

$$\frac{d}{dh} \left[e^{\frac{C_3 \rho_o - C_1}{C_2 \rho_o + C_1} \frac{gh}{V_z^2}} (V_{xw} - V_x) \right] = e^{\frac{C_3 \rho_o - C_1}{C_2 \rho_o + C_1} \frac{gh}{V_z^2}} \frac{dV_{xw}}{dh}. \quad (62)$$

Once again assuming a wind shear given by $V_{xw} = \alpha(h - h_o)$, we obtain:

$$\frac{d}{dh} \left[e^{\frac{C_3 \rho_o - C_1}{C_2 \rho_o + C_1} \frac{gh}{V_z^2}} (V_{xw} - V_x) \right] = \alpha e^{\frac{C_3 \rho_o - C_1}{C_2 \rho_o + C_1} \frac{gh}{V_z^2}},$$

or, after integrating,

$$e^{\frac{C_3 \rho_o - C_1}{C_2 \rho_o + C_1} \frac{gh}{V_z^2}} (V_{xw} - V_x) \Big|_{h=h_o}^{h=h} = \alpha \left[\frac{C_2 \rho_o + C_1}{C_3 \rho_o - C_1} \right] \frac{V_z^2}{g} e^{\frac{C_3 \rho_o - C_1}{C_2 \rho_o + C_1} \frac{gh}{V_z^2}} \Big|_{h=h_o}^{h=h},$$

at $h = h_o$, $V_{xw} - V_x = (V_{xw} - V_x)_o$ and thus we can solve this to obtain

$$(V_{xw} - V_x) - (V_{xw} - V_x)_o e^{-\frac{C_3 \rho_o - C_1}{C_2 \rho_o + C_1} \frac{g(h-h_o)}{V_z^2}} = \alpha \left[\frac{C_2 \rho_o + C_1}{C_3 \rho_o - C_1} \right] \frac{V_z^2}{g} \left[1 - e^{-\frac{C_3 \rho_o - C_1}{C_2 \rho_o + C_1} \frac{g(h-h_o)}{V_z^2}} \right] \quad (63)$$

which may be written as:

$$(V_{xw} - V_x) - (V_{xw} - V_x)_o e^{-f(h_o)(h-h_o)} = \frac{\alpha}{f(h_o)} \left[1 - e^{-f(h_o)(h-h_o)} \right], \quad (64)$$

where

$$f(h_0) = \frac{C_3 \rho_0 - C_1}{C_2 \rho_0 + C_1} \frac{g}{V_z^2} \quad (65)$$

Summarizing these two solutions, we have:

Solution I: Variable density, $V_z = \text{constant}$,

$$\begin{aligned} V_{xw} - V_x &= \frac{\alpha}{\beta(C_4 + 1) g(h)} \left\{ \left[1 + g(h) \left(\frac{\rho_0}{\rho} - 1 \right) \right]^{C_4 + 1} - 1 \right\} \\ q(h) &= 1 - \left(\frac{C_3}{C_2} + 1 \right) \frac{C_5 \rho}{1 + C_5 \rho} \end{aligned} \quad (66)$$

Solution II: Constant density, $V_z = \text{constant}$,

$$(V_{xw} - V_x) - (V_{xw} - V_x)_0 e^{-f(h_0)(h-h_0)} = \frac{\alpha}{f(h_0)} \left[1 - e^{-f(h_0)(h-h_0)} \right] \quad (67)$$

$$f(h_0) = \frac{C_3 \rho_0 - C_1}{C_2 \rho_0 + C_1} \frac{g}{V_z^2} \quad .$$

We shall now show that Solution II is approximately equal to Solution I for small altitude intervals. Expanding $g(h)$ and using the definition $C_5 = \frac{C_2}{C_1}$, we obtain:

$$\begin{aligned} g(h) &= \frac{1 + C_5 \rho - \left(\frac{C_3}{C_2} + 1 \right) C_5 \rho}{1 + C_5 \rho} \\ &= \frac{1 + \frac{C_2}{C_1} \rho - \left(\frac{C_3}{C_2} + 1 \right) \frac{C_2}{C_1} \rho}{1 + \frac{C_2}{C_1} \rho} = \frac{C_1 + C_2 \rho - \left(\frac{C_3}{C_2} + 1 \right) C_2 \rho}{C_1 + C_2 \rho} \\ &= \frac{C_1 - C_3 \rho}{C_1 + C_2 \rho} \quad . \end{aligned}$$

Therefore, we may write:

$$\beta(C_4 + 1) g(h) = \beta \left(\frac{g}{\beta V_z^2} + 1 \right) \frac{C_1 - C_3 \rho}{C_1 + C_2 \rho} \quad .$$

But $\frac{g}{\beta V_z^2} \gg 1$ and so we may write

$$\beta (C_4 + 1) g(h) = \frac{g}{V_z^2} \frac{C_1 - C_3 \rho}{C_1 + C_2 \rho}.$$

Thus we observe that:

$$\beta (C_4 + 1) g(h_0) = -f(h_0). \quad (68)$$

Using the experimental density law for small altitude intervals, we find:

$$\frac{\rho_0}{\rho} - 1 = \beta (h - h_0).$$

Thus, we have:

$$1 + g(h_0) \left(\frac{\rho_0}{\rho} - 1 \right) \cong 1 + g(h_0) \beta (h - h_0).$$

Also, for $h - h_0$ small, this represents the first two terms for the Taylor expansion of $e^{g(h_0)\beta(h-h_0)}$.

Thus we may write:

$$1 + g(h_0) \left(\frac{\rho_0}{\rho} - 1 \right) \cong e^{-\beta g(h_0)(h-h_0)}.$$

Or, for small altitude intervals we have:

$$\left[1 + g(h_0) \left(\frac{\rho_0}{\rho} - 1 \right) \right]^{C_4 + 1} \cong e^{\beta g(h_0)(h-h_0)(C_4 + 1)}.$$

Using relation (68) we have

$$\left[1 + g(h_0) \left(\frac{\rho_0}{\rho} - 1 \right) \right]^{C_4 + 1} \cong e^{-f(h_0)(h-h_0)}.$$

Thus, Solution I becomes:

$$V_{xw} - V_x = \frac{\alpha}{f(h_0)} \left[1 - e^{-f(h_0)(h-h_0)} \right]$$

which is identical to Solution II if $(V_{xw} - V_x)_0 = 0$.

Thus, we see that Solution II is of sufficient accuracy if $h - h_0$ is sufficiently small, i.e., if $(h - h_0) \leq 500$ ft.

C. Comparison of Analytical Solution with Computer Solution

As a check on the accuracy of Eqn 67 (Solution II), a comparison was made with computer solutions of Ref 2. These comparisons were made at large and small altitudes as well as large and small wind gradients. Figures 1, 2, and 3 present the solutions from Ref 2 as compared with Eqn 67. The solid curve was obtained from Ref 2 and represents a computer solution. The circled points were obtained from Eqn 67 with the apparent mass neglected ($K = 0$). The dashed curve was obtained from Eqn 67 with the apparent mass factor (K) assumed to be 0.5.

Comparison of the circled points with the solid curve indicates that Eqn 67 is extremely accurate for all altitudes and wind gradients. It is seen also that the wind response error is significantly increased due to the apparent mass characteristics of the balloon, consequently indicating that the apparent mass must not be neglected in problems of this nature.

h_0 = 15,000 ft. (4,570 meters)
 α = WIND GRADIENT = 0.14
 DIA. = 6 ft. (1.83 meters)
 WT. = 330 gms.
 GAS = HELIUM
 V_z = 13.9 meters/sec.
 (45.6 ft/sec)

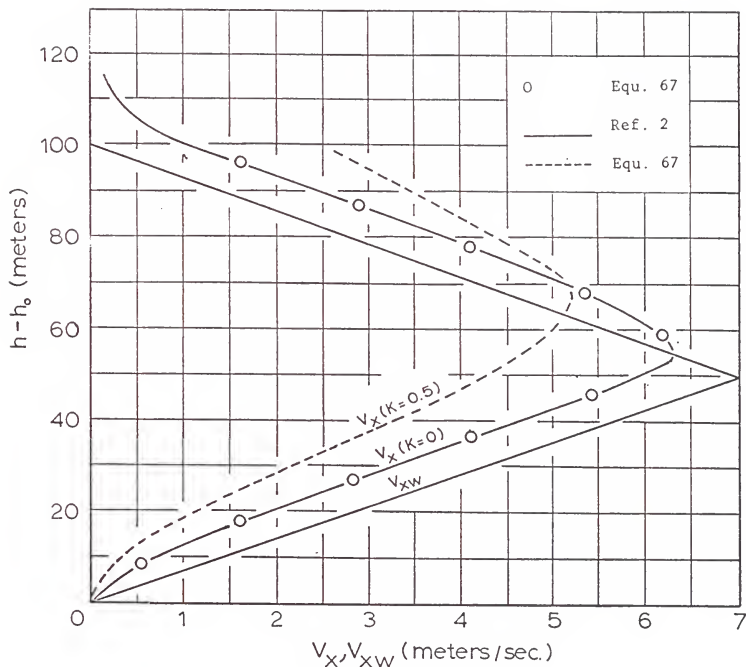


FIG 1. WIND SHEAR AND BALLOON VELOCITY
 (WITH APPARENT MASS FACTOR OF 0.0
 AND 0.5) AS A FUNCTION OF ALTITUDE
 ($h_0 = 15,000$ ft. , $\alpha = 0.14$)

h_0 = 15,000 ft. (4,570 meters)
 α = WIND GRADIENT = 0.28
 DIA. = 6 ft. (1.83 meters)
 WT. = 330 gms.
 GAS = HELIUM
 V_z = 13.9 meters / sec. (45.6 ft / sec.)

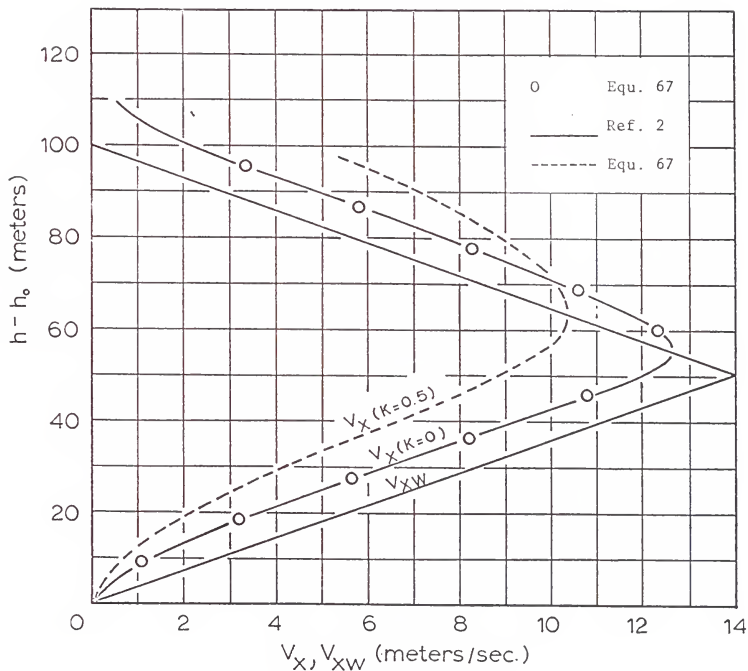


FIG 2. WIND SHEAR AND BALLOON VELOCITY
 (WITH APPARENT MASS FACTOR OF 0.0
 AND 0.5) AS A FUNCTION OF ALTITUDE
 ($h_0=15,000$ ft., $\alpha = 0.28$)

$h_o = 55,000 \text{ ft. (16,800 meters)}$
 $\alpha = \text{WIND GRADIENT} = 0.28$
 $\text{DIA.} = 6 \text{ ft (1.83 meters)}$
 $\text{WT} = 330 \text{ gms.}$
 $\text{GAS} = \text{HELIUM}$
 $V_z = 2.7 \text{ meters / sec. (8.85 ft / sec.)}$

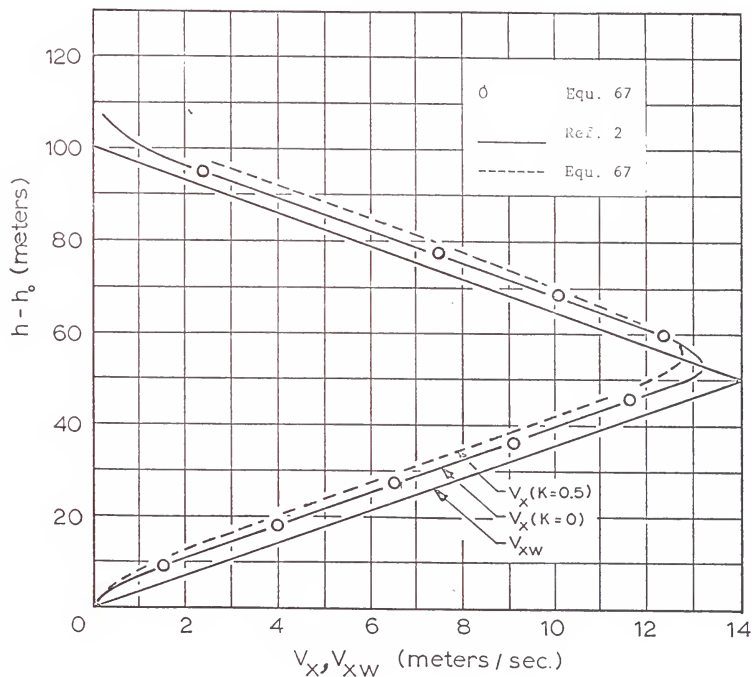


FIG 3. WIND SHEAR AND BALLOON VELOCITY
 (WITH APPARENT MASS FACTOR OF 0.0
 AND 0.5) AS A FUNCTION OF ALTITUDE
 ($h_o=55,000 \text{ ft.}, \alpha = 0.28$)

III. MEASUREMENT OF THE APPARENT MASS OF A SPHERE-LIKE BALLOON

1. Experimental Procedure

When a body moving in a fluid experiences an accelerating force, the reaction to this force is such that the change in velocity with time is slower than expected, appearing as if the body had a mass greater than the actual measured value. This experience is explained as the effect of the so-called "apparent mass", which has been calculated from potential flow equations for several relatively simple bodies. For several more complicated parachute-like bodies, the apparent mass has then been established experimentally (Ref 5).

A spherical balloon, used to measure winds as it rises through the atmosphere, experiences accelerations and decelerations as it passes through the layers of horizontal winds. The trajectory calculations of the preceeding chapter show that the apparent mass is of significant influence and must be considered in any determination of the wind pattern by means of an ascending balloon. Therefore, the objective of the following study is to establish experimentally the apparent mass for a wind-detecting balloon fabricated from flat gores and having an approximately spherical shape when properly inflated.

To measure the apparent mass of the balloons, experimental procedures were adopted as used in parachute technology (Ref 5). Modifying the referenced method for this purpose, the balloons were dropped from a height of about 25 feet in a hanger-like laboratory at the University of Minnesota. A known weight was suspended beneath the balloon and allowed to strike the floor. This impact provided an instantaneous deceleration of the balloon system while the drag of the system momentarily remained the same as before the impact. From this test procedure, the apparent mass can be determined in the following manner.

The forces acting on the balloon during the fall are shown in Fig 4. If the balloon is in steady state ($dv/dt = 0$) at this time, Newton's second law provides the following relation:

$$W_A + W_G + W_L + W_B - B - D = 0 \quad (69)$$

or

$$D = W_A + W_G + W_L + W_B - B \quad (70)$$

When the lost weight W_L strikes the floor, the equation of motion is

$$W_A + W_G + W_B - B - D = \left[\frac{W_A + W_G + W_B}{g} + m' \right] \frac{dv}{dt} \quad (71)$$

Solving for m' and considering the deceleration, dv/dt , to

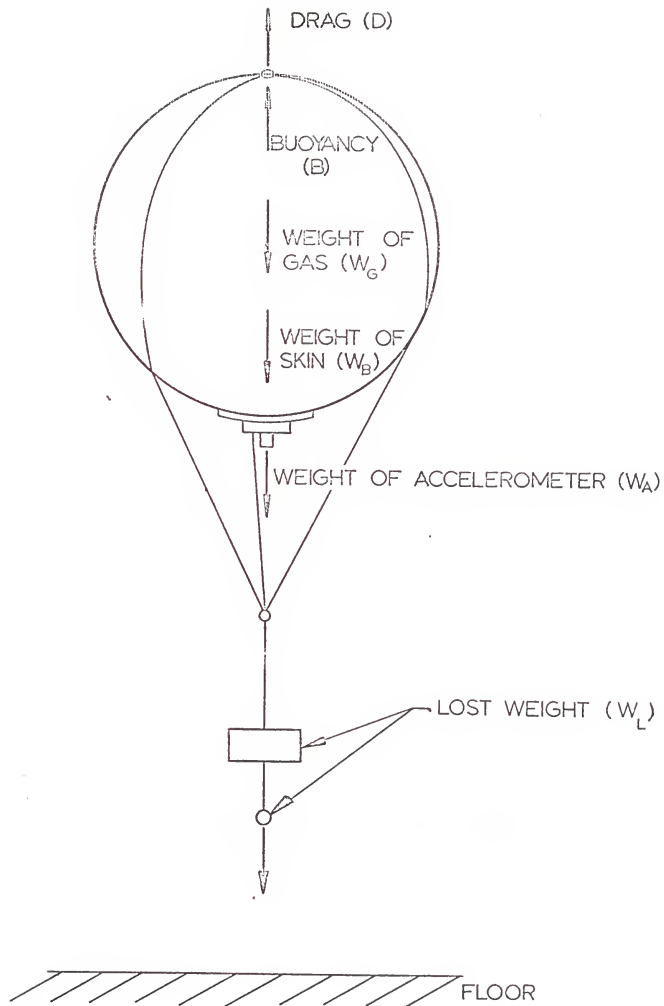


FIG 4. FORCES ACTING ON THE EXPERIMENTAL SYSTEM DURING DESCENT

be negative, we obtain

$$m' = \frac{W_L/g}{\frac{dv}{dt}} - \frac{W_A + W_G + W_B}{g} . \quad (72)$$

Multiplying by g to simplify later calculations, one obtains:

$$W' = \frac{W_L}{n} - (W_A + W_G + W_B) . \quad (73)$$

In the preceding analysis it was assumed that the balloon did not accelerate during its fall. However, in the actual case it was found that the balloon was still accelerated when the lost weight hit the floor. The equations of motion were modified accordingly. If we let a_0 be the acceleration of the balloon just previous to the impact of the lost weight, the equation of motion becomes:

$$W_A + W_G + W_L + W_B - B - D = \left[\frac{W_A + W_G + W_L + W_B}{g} + m' \right] a_0 . \quad (74)$$

The net weight of the balloon, F , is given by:

$$F = W_A + W_G + W_L + W_B - B . \quad (75)$$

This is a balance reading when the balloon system is set upon it, and hence is one of the measurements made during the test. If Eqn 75 is substituted into Eqn 74, we obtain

$$F - D = \left[\frac{W_A + W_G + W_B + W_L}{g} + m' \right] a_0 . \quad (76)$$

Using the new definition and after the weight strikes the floor, we have

$$F - D - W_L = \left[\frac{W_A + W_G + W_B}{g} + m' \right] \frac{dv}{dt} . \quad (77)$$

Solving for m' , we obtain

$$m' = \frac{F - D - W_L}{dv/dt} - \frac{W_A + W_G + W_B}{g} \quad (78)$$

Or, multiplying by g ,

$$W' = \frac{F - W_L - D}{n} - (W_A + W_G + W_B) \quad (79)$$

The right-hand side of Eqn 79 is easily determined, with the exception of the drag, D . Velocity measurements were made and the drag could be calculated from

$$D = \frac{1}{2} \rho V^2 C_D S \quad (80)$$

However, it was found that the Reynolds number of the experiments was close to the transitional range of a sphere, (3.45×10^5 and 1.77×10^5 for the 2.0 meter balloon; 2.60×10^5 and 1.31×10^5 for the 2.44 meter balloon), and the C_D values became somewhat uncertain.

In order to avoid detailed experiments to evaluate precise C_D 's for these models at the operating Reynolds numbers, a reiterative approximation process was used. Since a_0 is always small ($0.004 \leq a_0 \leq 0.022$ g's) one may assume that the balloon is in steady state before impact hence drag is known and we may calculate W' . Using this value and Newton's Second Law, we obtain from Eqn 74 a new drag term;

$$D = F - \frac{W_A + W_G + W_L + W_B + W'}{g} \cdot a_0 \quad (81)$$

Using this value for the drag and substituting it into Eqn 79,

one obtaining a new value for the apparent weight. Continued reiterations between Eqs 79 and 81 were performed until the value of W' changed in each process by less than 0.5%.

B. Models

The experimental system for apparent mass measurements consisted of a balloon, balloon rigging and weights, accelerometer, and a velocity measuring device (Fig 5).

1) Balloons

Two helium-filled balloons, constructed of 2 mil. mylar, were used in the tests. The larger balloon was 2.44 meters in diameter (8.0 feet) and the smaller balloon had a diameter of 2.0 meters (6.56 feet). The 2.44 meter balloon (Fig 6) had 24 gores and was nearly spherical. The 2.0 meter balloon (Fig 7) had only 12 gores and obvious deviations from spherical shape were observed (See Fig 8). The volume of this balloon was calculated assuming the balloon was composed of several special ungulas of a right circular cylinder.

In preliminary work, the balloons were filled to a specific inflation pressure with air. With this arrangement, the mass of the system became extremely large and since the mass of the included gas must be considered in the calculations of acceleration, it appeared necessary to reduce

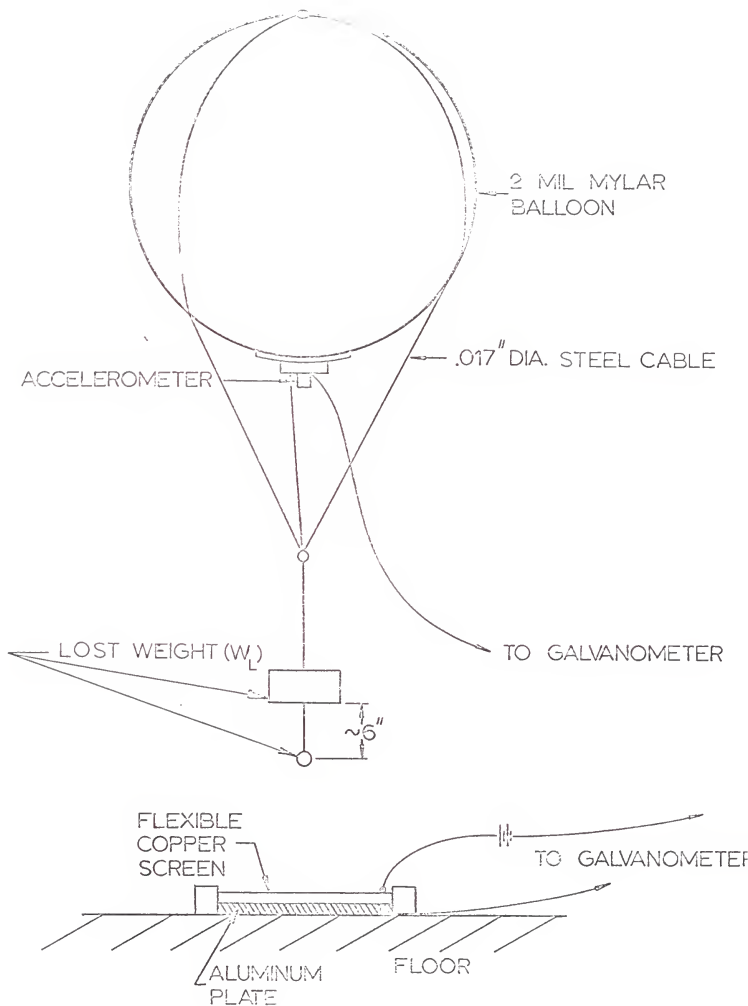


FIG 5. SCHEMATIC DIAGRAM OF TEST APPARATUS AND ARRANGEMENT

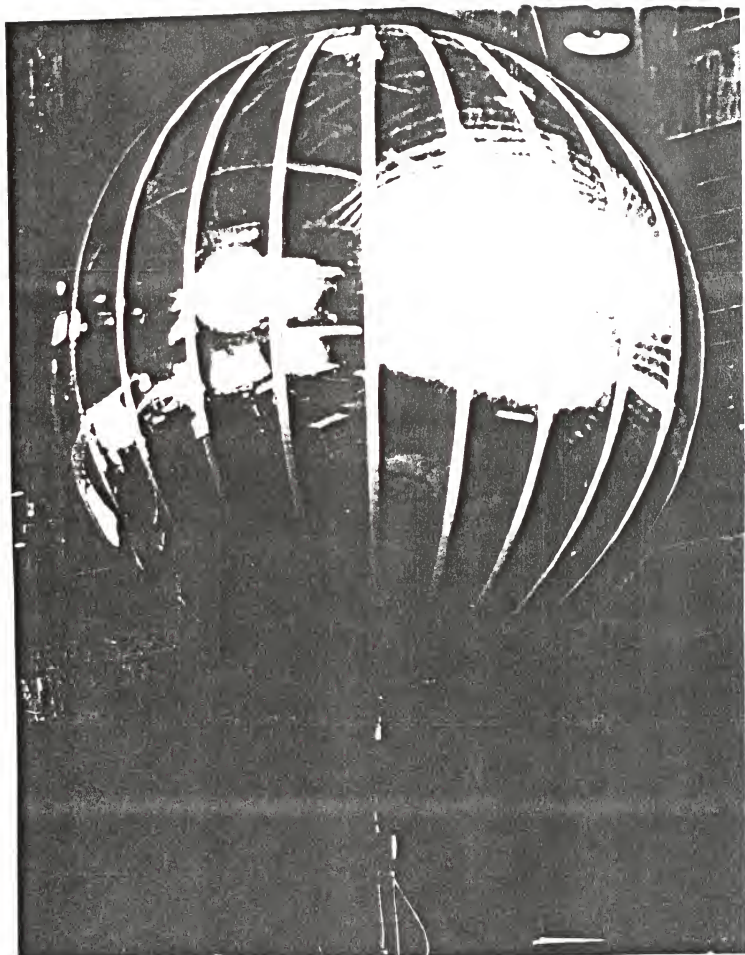


FIG 6. PHOTOGRAPH OF INFLATED 2.44
METER BALLOON (24 GORES)

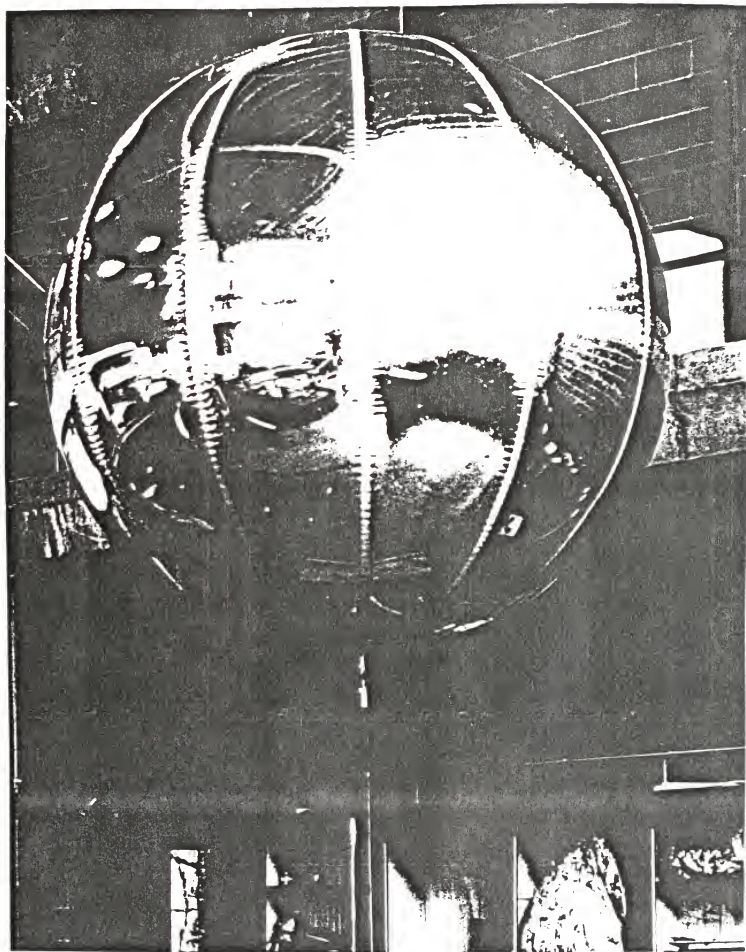


FIG 7. PHOTOGRAPH OF INFLATED 2
METER BALLOON (12 GORES)

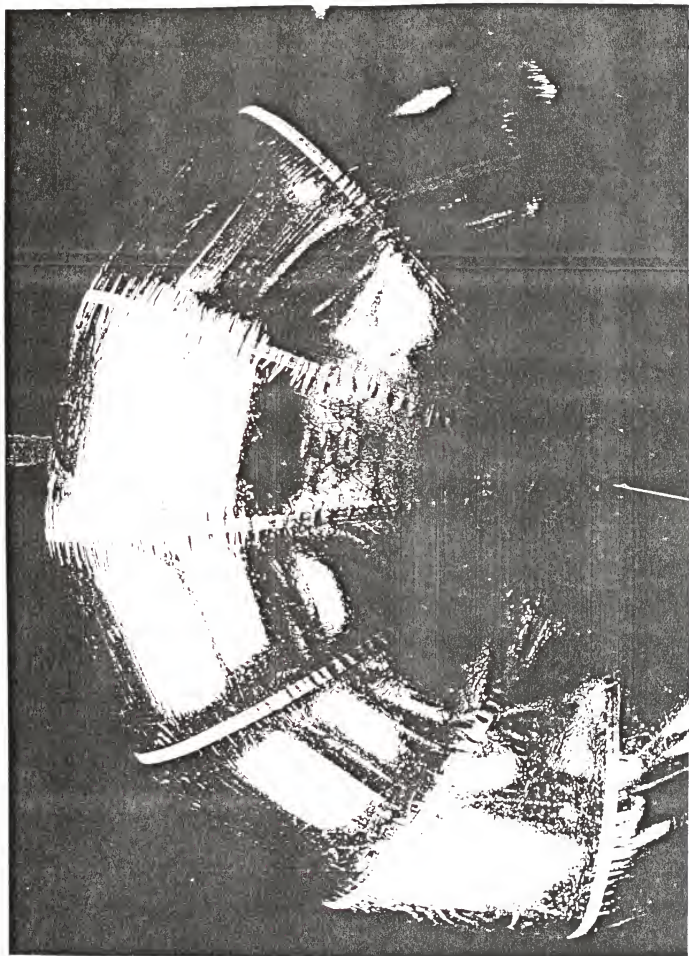


FIG 8. INFLATED 12 GORE BALLOON SHOWING
NONSPHERICITY OF CROSS-SECTION

the system mass by introducing a lighter gas into the balloon.

Using helium, the balloons developed a free lift of $5\frac{1}{2}$ lbs for the 2.0 meter balloon and $9\frac{1}{2}$ lbs for the larger one. Then using a lost weight of six(6) and ten(10) lbs, respectively, the resultant downward force, the system's mass, and its drag were considerably decreased. This greatly simplified test procedure, calculations, and reduced the probability of accelerometer damage due to excessive loads and rebound acceleration.

Using this system, the lost weight could easily be varied, causing impact velocities and Reynolds number to vary in the desired manner.

2) Balloon Rigging and Weights

The balloon rigging consisted of a harness of three 0.017 inch steel cables, equispaced over the balloon surface, fastened together at the top and meeting at a confluence point below the balloon and supporting the "lost" weight (Fig 5).

3) Accelerometer

A Statham accelerometer with a range of ± 3 g's was used to measure all accelerations of the balloon system. The accelerometer was fastened to an aluminum sphere section

of 14 inch chord length which was attached to the base of the balloon. This arrangement formed a rigid system of balloon, plate, and accelerometer. In preliminary work the accelerometer was suspended by a single cord a few inches below the balloon. This suspension was unsatisfactory because the accelerometer became excited from vibrations of the balloon when the lost weight contacted the floor and the static and dynamic equilibrium of the balloon was disturbed.

4) Velocity Indication

The velocity of the descending balloon had to be measured prior to ground impact. For this purpose the following method was employed: A copper screen was stretched $\frac{1}{4}$ inch above an aluminum plate and both surfaces were placed on the floor. The plate and the screen were connected to a Century oscillograph which recorded the instant of contact between the screen and the aluminum plate. The time base of the Century read-out system was used to measure the interval between the instants at which a small steel ball, suspended beneath the main part of the lost weight, and the main portion of the lost weight itself contacted the wire screen.

The ball was heavy enough to depress the screen upon impact, but light enough to allow the screen to break

contact with the ground plate. The lost weight provided the permanent deflection shown in the oscillogram.

4) Data Recording

The accelerations and velocity indications were recorded and a sample trace is shown in Fig 9. Note that the balloon acceleration, is averaged over a finite time period. This is permissible since the aerodynamic drag, which changes with the velocity, is small compared with the other terms of the system shown in Eqn 69.

C. Results

A summary of results is presented in Table 1 and Fig 10. The value of K, defined as

$$K = \frac{m'}{B} ,$$

is predicted by potential flow theory to be 0.500 for a sphere (Ref 3). As is shown in the table, the experimental values are quite close to this analytically derived value. Reviewing the results, one notices in the table as well as in the graph a trend of increasing apparent mass with decreasing Reynolds number . This may be explained as being a consequence of the varying flow pattern. It was mentioned that the 2.0 meter balloon deviates more from the spherical form

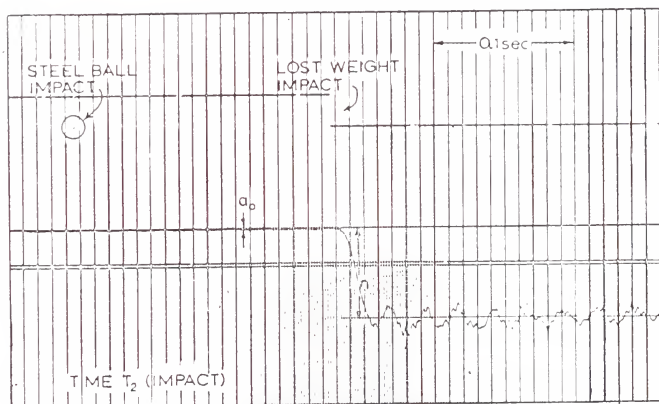
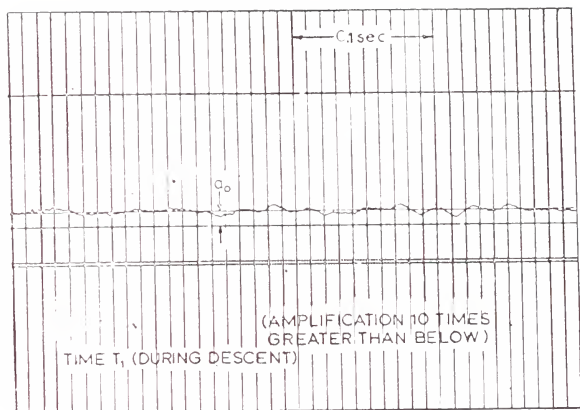


FIG. 9. SAMPLE OSCILLOGRAPH TRACE

SPHERE DIAMETER (ft.)	6.56 (2 METER)	6.56 (2 METER)	8 (2.44 METER)	8 (2.44 METER)
SPHERE VOLUME (ft.) ³	141.2	141.2	268.1	268.1
REYNOLDS NO.	345,000	177,000	260,000	131,000
IMPACT VELOCITY (ft./sec.)	7.1	4.5	5.4	2.7
AVERAGE IMPACT DECELERATION (g's)	0.548	0.503	0.467	0.461
AVERAGE DESCENT ACCELERATION (g's)	0.022	0.004	0.022	—
C _D , DRAG COEFFICIENT*	0.119	0.182	0.074	—
K = $\frac{\text{APPARENT MASS}}{\text{BUOYANCY}}$	0.519	0.550	0.485	0.512

* ESTIMATED

TABLE I. EXPERIMENTAL RESULTS AT VARIOUS REYNOLDS NUMBERS FOR A FREELY DESCENDING SPHERE

than the larger one. This difference in the shape could account for the 7% difference in the apparent mass factor K for the two balloons. Since K for a cube is 0.670 (Refs 5 and 6), and the projection of the 2.0 meter model is more polygonal, an apparent mass factor higher than the one for a sphere appears to be reasonable.

IV. CONSLUSIONS

The trajectory calculations in Section II illustrate the response error and the pertinent equations show the terms which essentially cause the lack of motion of the balloon behind the actual wind. Results show that the apparent mass is a significant factor and must be included in the analysis of such a system (Figs 1 through 3). For this analysis, a theoretically derived value of $K = 0.5$ was used as the apparent mass factor.

The trajectory calculations described in Section II compare favorably with computer solutions. The more exact calculations as well as the solution of the equation of motion appear to be acceptable for use in data evaluation.

An analysis of the wind response equations (Eqn No 67) shows that a minimum error can be obtained if the following criteria are considered:

- 1) The balloon should rise as slowly as possible.
- 2) The apparent mass factor K is of importance and must be kept as small as possible.
Also examination of relation (14) indicates that:
- 3) The ratio of the weight to drag, $W/C_D S$, should be a minimum.

In addition to these considerations are several other items such as size for radar soundings and balloon strength and shape. The pursuit of these circumstances exceeds the scope of this study.

The apparent mass factor used in the calculations

was assumed to be $K = 0.5$. Experiments showed that the apparent mass factor of actual balloons is close to the theoretical value. A certain dependency (Table I, Fig 10) of the apparent mass factor upon Reynolds number is indicated, but under the scope of the present program this phenomenon was not investigated further.

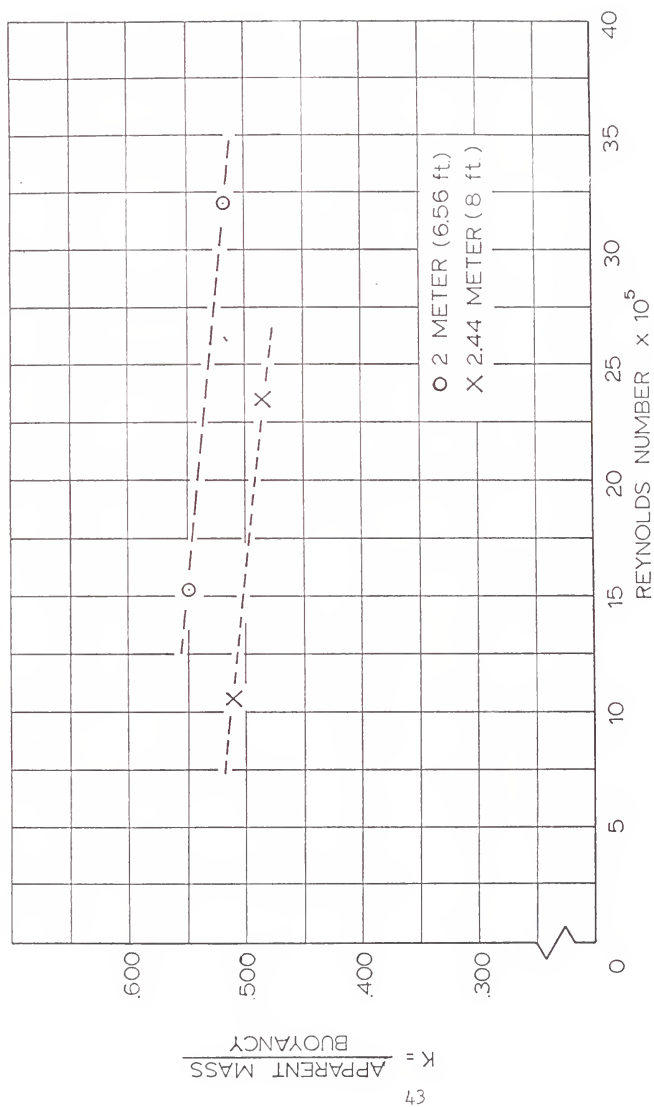


FIG 10. APPARENT MASS FACTOR VS. REYNOLDS NO. FOR
SUPER PRESSURIZED MYLAR BALLOONS

REFERENCES

1. Leviton, R.: A Detailed Wind Profile Sounding Technique, proceedings of the National Symposium on Winds For Air-Space Vehicle Design, Air Force Surveys in Geo-Physics No 140, Geophysics Research Directorate, Bedford, Mass., March 1952, pp. 187-196.
2. Johnston, K. D.: Response of Spherical Balloon to Wind Gusts, George C. Marshall Space Flight Center, Huntsville, Alabama, March 5, 1962, Memo M-AERO-A-12-62.
3. Lamb, Sir Horace: Hydrodynamics, Dover Publications, New York, Sixth Edition, 1932.
4. Rust, L. W., Jr.: Trajectory Analysis of a Vehicle Entering a Planetary Atmosphere With Analytical and Numerical Solutions, Master's Thesis, University of Minnesota, July, 1961.
5. Heinrich, H. G.: Experimental Parameters in Parachute Opening Theory, Bulletin of the 19th Symposium on Shock and Vibration, 1953, Office of the Secretary of Defense, Washington, D. C.
6. Stelson, J. F. and Davis, F. T.: Virtual Mass and Acceleration in Fluids, Translation, ASCE, Vol. 22, 1957, pp. 518-530.
7. Heinrich, H. G. and Ibrahim, S. K.: Experimental Determination of the Apparent Moment of Inertia of Parachutes, University of Minnesota, 1963, in printing.
8. Zahm, A. F.: Flow and Force Equations for a Body Revolving in a Fluid, Parts IV and V, NACA TR 323, 1929.
9. Durand, W. F.: Aerodynamic Theory, Vol I, Durand Re-printing Committee, 1943.

